angle S2-P-O3 is opened up to 124.35 (8)°, the axial atoms are tipped away from these atoms toward O2 for an angle S1-P-O1 of 177.38°.

Conclusion. With regard to ring orientation, the study of new oxyphosphoranes possessing sulfur rings and pentafluorophenoxy ligands leads to axial-equatorial ring placement in TBP geometries similar to that found in other studies with cyclic pentaoxyphosphoranes.[4-10,18] Thus far, use of electronegative ligands, steric and hydrogen bonding[4] effects, introduction of trans-fused rings,[10] or varying ring size from five- to eight-membered[8,9] has not yielded a solid-state structure of a pentacoordinated phosphorus molecule displaying diequatorial ring occupancy. However, use of these variations has led to the formation of chair conformations[4] in addition to the more prevalent boat form[7-10] for phosphorinane rings in axial-equatorial sites of TBP geometries. In the present study, the unique chair conformation found for the six-membered ring of **1** had a short P-O axial bond equal in length to the P-O equatorial bond within the accuracy of the measurement, the first observation of this kind in pentacoordinated phosphorus chemistry. Future work on structural preferences of cyclic oxyphosphoranes should prove valuable in assisting mechanistic studies of *c*-AMP action and more generally in interpreting mechanisms of reaction of cyclic phosphates.

Acknowledgment. The support of this research by the National Science Foundation (Grant CHE 88-19152) and the Army Research Office is gratefully acknowledged.

Supplementary Material Available: Tables of atomic coordinates, thermal parameters, additional bond lengths and angles, and hydrogen atom parameters (Tables S1-S4 for **1**, Tables S5-S8 for **2**, and Tables S9-S12 for **3**) (24 pages); listings of observed and calculated structure factors for **1-3** (28 pages). Ordering information is given on any current masthead page.

Contribution from the Department of Chemistry,
Wayne State University, Detroit, Michigan 48202

Stereochemical Perturbations of the Relaxation Behavior of (^{2}E)Cr(III). Ground-State X-ray Crystal Structure, Photophysics, and Molecular Mechanics Simulations of the Quasi-Cage Complex [4,4′,4″-Ethylidynetris(3-azabutan-1-amine)]chromium Tribromide[1]

Marc W. Perkovic, Mary Jane Heeg, and John F. Endicott*

Received September 18, 1990

The X-ray crystal structure of $Cr(sen)^{3+}$ (sen = 4,4′,4″-ethylidynetris(3-azabutan-1-amine)) demonstrates that the coordination environments are very similar in this complex and $Cr(en)_3^{3+}$. However, the photophysical behaviors of these complexes contrast markedly, with $Cr(sen)^{3+}$ having a much shorter ^{2}E excited-state lifetime (by a factor of at least 10^4) in ambient fluid solutions. The bond angles of the neopentyl cap (N-C-C and CH_2-C-CH_2) of $Cr(sen)^{3+}$ are 5-10° larger than normal, and this is attributed to trigonal strain in the ligand induced by coordination to Cr(III). MM2 calculations indicate that coordination geometry preferred by the ligand would be very nearly halfway between the ideal prismatic and antiprismatic microsymmetries. In contrast to the fluid solution behavior, (^{2}E)$Cr(sen)^{3+}$ doped into $[Rh(sen)](ClO_4)_3$ was found to have a 13-μs lifetime at 298 K. The facile, thermally activated fluid solution excited-state relaxation channel is attributed to a large amplitude ligand-promoted trigonal twist of the electronically excited complex. $[Cr(sen)]Br_3$, $CrN_6C_{11}H_{30}Br_3$, crystallizes in the monoclinic space group $P2_1/c$ with Z = 4 and a = 13.964 (4) Å, b = 10.777 (2) Å, c = 13.027 (3) Å, and β = 98.34 (2)°. The structure refined to R = 0.055 and R_w = 0.050 with 1612 observed reflections.

Introduction

Transition-metal excited states have considerable potential for use as chemical reagents or as key elements in optoelectronic systems.[2-4] Realization of this potential often requires that excited-state electronic configurations persist for appreciable time periods when the conditions are ambient or nearly ambient. However, the ambient lifetimes of transition-metal excited states are usually dictated by poorly understood thermal deactivation processes. Chromium(III) complexes nicely illustrate the problems involved, since the decay of the lowest energy excited state, (^{2}E)Cr(III), is spin forbidden and does not involve a change of orbital electronic population. As a consequence, the ^{2}E excited state and the $^4A_2$ ground state have very nearly identical molecular geometries, and the excited-state lifetime should be dictated by nearly temperature-independent tunneling processes.[5,6] Yet (^{2}E)Cr(III) excited-state lifetimes are usually strongly temperature dependent in ambient fluid solutions and lifetimes in the subnanosecond regime are not uncommon.[5] The observed relaxation behavior can be represented as

$$\tau^{-1} = k = k_{lim} + k(T) \quad (1)$$

where τ is the observed mean lifetime,[7,8] k_{lim} is the limiting low-temperature (nearly temperature independent) relaxation rate constant, and $k(T)$ represents the thermally activated relaxation behavior. For (^{2}E)Cr(III) excited-state decay, $k(T)$ has been found to increase monotonically with temperature[5] and it is often fitted to a simple Arrhenius function, $k(T) = A\exp(-E_a/RT)$.[9,10] This behavior is suggestive of simple chemical reactions in which a reactant must acquire thermal energy sufficient to allow the changes in molecular geometry (including necessary changes in position of solvent, as well as reactant nuclei) necessary to generate the transition-state characteristic of the reaction process.[5a] However, there are usually several possible, perhaps competing, pathways for the thermally activated decay of electronically excited molecules.[5a,8,10] Thus, for Cr(III) complexes several distinct

(1) We gratefully acknowledge the Division of Chemical Sciences, Office of Energy Research, U.S. Department of Energy for partial support of this research.
(2) Balzani, V.; Moggi, L. *Coord. Chem. Rev.* **1990**, *97*, 313.
(3) Hopfield, J. J.; Onuchic, J. N.; Beratan, D. N. *J. Phys. Chem.* **1989**, *93*, 6350.
(4) Gütlich, P.; Hauser, A. *Coord. Chem. Rev.* **1990**, *97*, 1.
(5) For reviews, see: (a) Endicott, J. F.; Ramasami, T.; Tamilarasan, R.; Lessard, R.; Ryu, C. K.; Brubaker, G. R. *Coord. Chem. Rev.* **1987**, *77*, 1-87. (b) Forster, L. S. *Chem. Rev.* **1990**, *90*.
(6) Important features of (^{2}E)Cr(III) excited-state relaxation in the low-temperature regime (k_{lim}) are examined in detail elsewhere: (a) Ryu, C. K.; Lessard, R. B.; Lynch, D.; Endicott, J. F. *J. Phys. Chem.* **1989**, *93*, 1752. (b) Endicott, J. F.; Lessard, R. B.; Lynch, D. L.; Perkovic, M. W.; Ryu, C. K. *Coord. Chem. Rev.* **1990**, *97*, 65.
(7) The (^{2}E)Cr(III) decays have often been observed to be biexponential,[5b,8] so eq 1 should be regarded as somewhat idealized. The fluid solution lifetimes of the complexes reported in this paper fit single exponential behavior reasonably well.
(8) Forster, L. S.; Murrow, D.; Fucaloro, A. F. *Inorg. Chem.* **1990**, *29*, 3706.
(9) Non-Arrhenius behavior has sometimes been observed,[5] and it has also been suggested that $k(T)$ might approach a high-temperature-limiting value for some complexes.[10]
(10) Lessard, R. B.; Endicott, J. F.; Perkovic, M. W.; Ochromowycz, L. M. *Inorg. Chem.* **1989**, *28*, 2574.

0020-1669/91/1330-3140$02.50/0

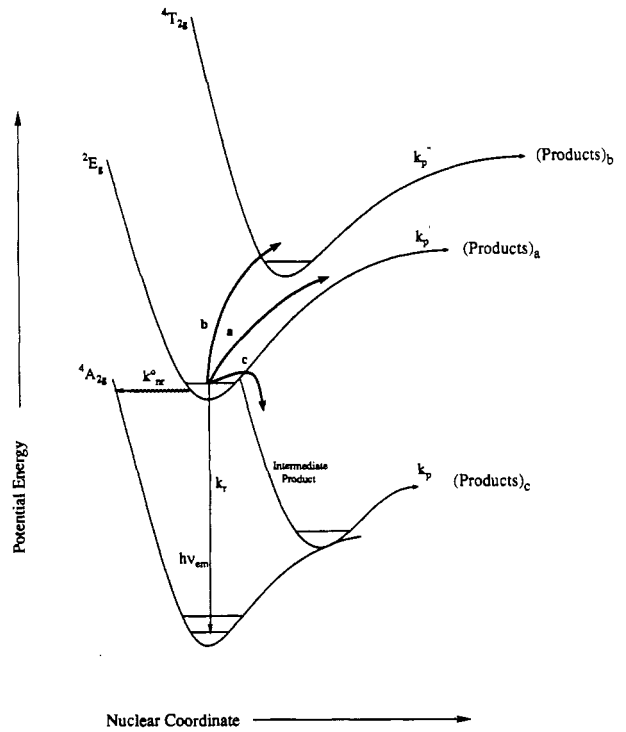

Figure 1. Qualitative illustration of mechanisms proposed for thermally activated (^{2}E)Cr(III) excited-state relaxation: (a) direct reaction to form electronically correlated products; (b) back intersystem crossing; (c) crossing to the potential energy surface of a ground-state intermediate. The "products" indicated may or may not differ chemically from the original ground state. In principle, each of the mechanistic pathways could involve a different nuclear coordinate(s), but only one coordinate is indicated for simplicity. These mechanisms for thermally activated (^{2}E)Cr(III) relaxation have been proposed to account for $k(T)$, where the observed relaxation rate constant is $k = k_{lim} + k(T)$ and $k_{lim} = k_r + k_{nr}^o$.

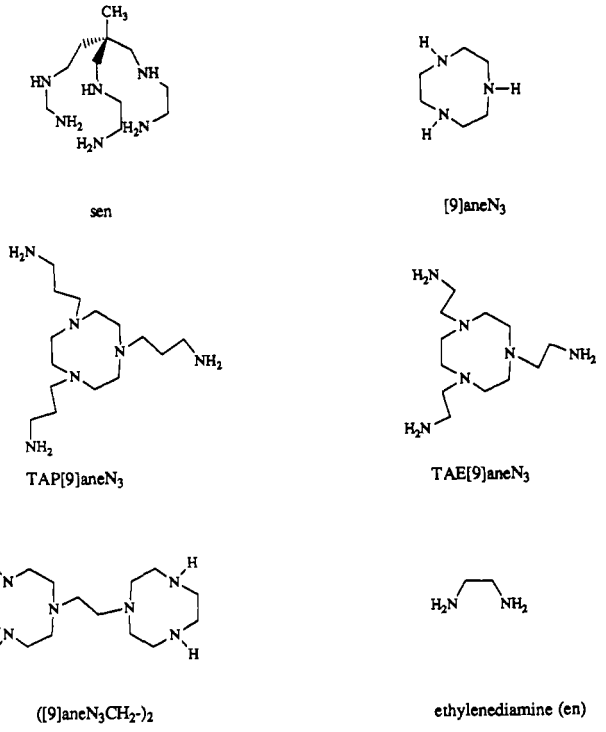

Figure 2. Skeletal structures of ligands.

mechanisms have been proposed to account for the thermally activated nonradiative relaxation of the ^{2}E excited states:[5a,11] (a) direct chemical reaction;[12] (b) back intersystem crossing to a quartet excited state;[11,13,14] (c) excited state to ground state chemical intermediate surface crossing.[5a,15] It now seems unlikely that any one of the mechanisms proposed is adequate to describe $k(T)$ for all Cr(III) complexes,[5,8,10] and it is likely that for some complexes the observed $k(T)$ represents the sum of these and possibly other kinetically competitive pathways for (^{2}E)Cr(III) relaxation. The three noted thermal relaxation pathways are qualitatively illustrated in Figure 1. From this point of view, the mechanistically useful studies would be those that explore one hypothetical relaxation channel while minimizing (or at least holding constant) the contributions of others.

Much of our recent work has been directed toward elucidation of the third of these (i.e., mechanism c above) proposed thermally activated (^{2}E)Cr(III) relaxation channels.[5a,6b,10,16,17] The surface crossing mechanism postulates a thermally activated nuclear distortion that mixes orbital character and/or increases spin–orbit coupling, thereby reducing some of the forbidden character of the excited-state relaxation process. An implication of this mechanism is that stereochemical factors should play an important role in dictating (^{2}E)Cr(III) excited-state lifetimes. There is accumulating evidence that this is the case.[10,16,17,18] This paper is the first full report of our studies of the effects of stereochemical perturbations on $k(T)$ in closely related pairs of hexaamine complexes.[19] Hexaamine complexes have been chosen for this work because (a) a large variation in stereochemical perturbations is possible and (b) the contributions of the back intersystem crossing pathway (i.e., mechanism b above) ought to be minimized in this class of complexes.[5,8,10] We have sought to further minimize any complications arising from back intersystem crossing through the careful pairwise comparison of complexes with very similar electronic structures.

Since the energy of the (^{2}E)Cr(III) electronic excited state usually exceeds the energy requirements for one or more of the possible transition states for ground-state substitution, we some time ago postulated[5a,16] that certain of these transition states for ground-state substitution might appear as "metastable intermediates" along an excited-state relaxation pathway and that such a relaxation coordinate could be analogous to the thermally activated spin relaxation of transition-metal complexes in which the two spin states differ greatly in geometry.[20–22] One such pathway that we suggested[5a,10] might account for certain peculiarities in reported (^{2}E)Cr(III) relaxation behavior was a thermally activated trigonal twist.

Trigonal distortions are a particularly interesting subset of the nuclear motions that might be effective in mixing d-orbital electronic configurations, since (a) such motions map into the low-frequency t_{2u} twisting mode for octahedral Cr(N$_6$) symmetry ($\nu_{t2u} \cong 200$ cm^{-1} in Cr(NH$_3$)$_6^{3+}$ [5a]), so that large amplitude motions involving several quanta in such modes could contribute to an activation barrier under ambient conditions ($k_BT = 206$ cm^{-1}), (b) such motions effectively mix nonbonding and bonding d-orbital character and (c) they mix d- and p-orbital character,[23] (d) the

(11) Kirk, A. D. *Coord. Chem. Rev.* **1981**, *39*, 225.
(12) Gutierrez, A. R.; Adamson, A. W. *J. Phys. Chem.* **1978**, *82*, 902.
(13) Balzani, V.; Carassiti, V. *Photochemistry of Coordination Compounds*; Academic: London, 1970.
(14) Linck, N. J.; Berens, S. J.; Magde, D.; Linck, R. G. *J. Phys. Chem.* **1987**, *26*, 2334.
(15) Endicott, J. F.; Ferraudi, G. J. *J. Phys. Chem.* **1976**, *80*, 949.
(16) Endicott, J. F.; Lessard, Y.; Ryu, C. K.; Tamilarasan, T. In *Excited States and Reactive Intermediates*; Lever, A. B. P., Ed.; ACS Symposium Series No. 307; American Chemical Society: Washington, DC, 1986.
(17) Perkovic, M. W.; Endicott, J. F. *J. Phys. Chem.* **1990**, *94*, 1217.
(18) (a) Kane-Maguire, N. A. P.; Crippen, W. S.; Miller, P. K. *Inorg. Chem.* **1983**, *22*, 696. (b) Kane-Maguire, N. A. P.; Wallace, K. C.; Miller, D. B. *Inorg. Chem.* **1985**, *24*, 597.
(19) Preliminary reports of our observations on the two other pairs of complexes in this series have appeared elsewhere: (a) Cr([9]aneN$_3$)$_2^{3+}$ and Cr([9]aneN$_3$CH$_2$-)$_2^{3+}$;[6b] (b) Cr(TAP[9]aneN$_3$)$^{3+}$ and Cr(TAE[9]-aneN$_3$)$^{3+}$.[17]
(20) For a review, see: Beattie, J. K. *Adv. Inorg. Chem.* **1988**, *32*, 1.
(21) Dose, E. V.; Hoselton, M. A.; Sutin, N.; Tweedle, M. F.; Wilson, L. J. *J. Am. Chem. Soc.* **1978**, *100*, 1141.
(22) Buhks, E.; Navon, G.; Bixon, M.; Jortner, J. *J. Am. Chem. Soc.* **1980**, *102*, 2918.

trigonal prismatic "intermediate" species, which would be the ultimate product of such distortions, need not lead to net chemical reactions, and (e) doubly occupied microstates contribute to the (^{2}E)Cr(III) wave function in trigonally distorted Cr(III) complexes[24] and this should make the metal–ligand electronic repulsions for distortions along a trigonal coordinate smaller in the ^{2}E excited state than in the $^4A_2$ ground state.

We have been examining the photophysical behavior of several trigonally strained (hexaamine)chromium(III) complexes.[6b,17] Overall, these complexes differ only a little in their excited-state energies, but they span a range of more than 10^8 in their (^{2}E)-Cr(III) lifetimes in ambient, fluid solutions. In this report we describe a particularly simple example of the behavior of this family of complexes in the contrast between the ambient photophysics of $Cr(en)_3^{3+}$ and $Cr(sen)^{3+}$,[25] where the sen complex can be viewed as a $Cr(en)_3^{3+}$ complex capped at a trigonal face by a neopentyl group (see Figure 2).

Experimental Section

$[Cr(en)_3](ClO_4)_3$ was prepared by recrystallization of the commercially available chloride salt in dilute aqueous perchloric acid (ca. 0.01 M) by the addition of solid $NaClO_4$. *Caution! Perchlorate salts of chromium(III) amines are potentially explosive.*

[Cr(sen)]Br$_3$. The ligand sen was prepared as described in the literature.[26] The oil was purified by vacuum distillation (method two in ref 26). The chromium(III) complex was prepared by boiling 1.0 g of $CrCl_3 \cdot 6H_2O$ in 10 mL of dimethylformamide (DMF) for 15 min. Next, 1.0 g of sen oil in 5 mL of boiling DMF was added and the mixture was stirred at a gentle boil for 30 min. Upon cooling, a brick red solid was collected by suction filtration, and the desired yellow product crystallized from an aqueous solution of the red solid following the addition of NaBr. The bright yellow solid that resulted was recrystallized from water and air-dried. The final yield was 0.6 g (30%) of X-ray-quality crystals. Authenticity was based on the UV–vis spectrum[27] in water (λ, nm (ϵ, M^{-1} cm^{-1}): 347 (65), 451 (97)) and, ultimately, the X-ray structure.

[Rh(sen)]Cl$_3$. Rhodium trichloride hydrate (Johnson Mathey, 237 mg) and the free-base sen (297 mg) were mixed in 15 mL of dry methanol and heated to a gentle boil. The initially red-brown solution quickly began to lighten in color, and a fine, white precipitate was observed. After 30 min the now yellow solution was cooled to 0 °C and the solid collected by suction filtration. The white solid was washed with ice-cold methanol and air-dried. Recrystallization from an aqueous solution of NH_4Cl yielded 109 mg (21%) of a white, microcrystalline solid. Anal. Calc (found) for $C_{11}H_{30}N_6RhCl_3$: C, 21.76 (21.87); H, 5.31 (5.06); N, 13.84 (13.90). The bromide salt was prepared by recrystallization of the chloride salt from an aqueous HBr/NaBr solution.

The doped solid was prepared by dissolving a 1:30 molar ratio (Cr:Rh) of the sen complexes in hot water followed by precipitation with solid $NaClO_4$.

Luminescence spectra were recorded after excitation by the 437-nm radiation from a molectron UV1010 nitrogen laser pumped DL 14 dye laser on a Princeton Instruments IRY512 diode array with an ST120 controller. Luminescent lifetimes were determined by using a Gould Biomation 4500 digital (10 ns/sample) oscilloscope/Hammamatsu R955 PMT instrument. Both instruments were interfaced to a PC/AT computer. Kinetic data was analyzed by using the KINFIT package from On-Line-Instrument-Systems, Jefferson, GA. Further details of the instrumentation may be found in ref 12b.

Table I. Experimental Crystallographic Data for $[Cr(sen)]Br_3$

formula	$Cr_1N_6C_{11}H_{30}Br_3$
color, habit	yellow plates
mol wt	538.11
density (calc), g cm^{-3}	1.843
cryst dimens, mm	0.28 × 0.24 × 0.10
cryst system	monoclinic
space group	$P2_1/c$
cell dimens	
a, Å	13.964 (4)
b, Å	10.777 (2)
c, Å	13.027 (3)
β, deg	98.34 (2)
V, Å^3	1939.7 (8)
Z	4
scan method	$\theta/2\theta$
scan range, deg	1.0 below $K\alpha_1$, 1.0 above $K\alpha_2$
scan rate, deg min^{-1}	2–5, variable
bkgd/scan time	0.5
2θ range, deg	6–52
h, k, l ranges	$0 \le h \le 18$
	$0 \le k \le 14$
	$-17 \le l \le 17$
tot. no. of data	4338
no. of obsd data, $I_0 \ge 3\sigma(I)$	1612
μ (cm^{-1})	67.0
transm coeffs	0.922–0.394
$F(000)$	1068
R, R_w	0.055, 0.050
w	$(\sigma_F^2 + 0.0002F^2)^{-1}$

Quantum yields were determined by using a frequency-tripled Quantel Model 661 Nd-YAG laser (355 nm) as pump and a PRA LN-103 N_2-laser pumped LN-102 dye laser (520 nm) as a probe. The probe beam was sampled before and after the sample with Molectron LP131 integrating photodiode detectors. The detector outputs were fed into two Evans Electronics 4103A sample and hold, low leakage, gated integrators, which functioned as rudimentary boxcar integrators. The integrator voltages were read, the pump-probe delay controlled, and the whole system operated by using customized software developed in house in collaboration with On-Line Instrument Systems, Inc. (OLIS, Jefferson, GA) and a Zenith Z158 computer. Further details of this system will be presented elsewhere. Quantum yields were determined from changes in absorbance at 530 nm with the number of pump pulses by using the molar absorptivities (at 530 nm) of the substrate and the photolysis product. We used $Cr(NH_3)_6^{3+}$ to calibrate the system. Quantum yields were based on the initial slopes of plots of absorbance change vs the number of pulses.

Molecular mechanics calculations were performed on an AT&T 3B2/310 computer using a locally modified[28] version of the Allinger–Yuh MM2/MMP2 program.[29] The calculational protocol was designed to assess the change in the coordinated amine ligand steric energy (residual energy) as the N–Cr–N moieties were exercised through various angles and/or perturbed by the addition of a water molecule to the coordination sphere. Atomic parameters for the organic moieties were those of the MM2 force field. For the metal–ligand interactions the values of Brubaker and Johnson[30] were used. Initial atomic coordinates were those of the orthogonalized X-ray coordinates. The choice of unstrained coordination sphere M–L bond lengths and angles were based on the $Cr(NH_3)_6^{3+}$ paradigm (2.06 Å for Cr–N) and 90 and 180° for N–Cr–N angles. The calculations assumed that there was no electron delocalization in the molecule and that the metal had no effect on nonligating atoms. No formal charge was assigned to the Cr(III) ion; however, the M–L dipoles were assigned, on the basis of optical electronegativities, and this partly corrected for the effects of a heteroelectrical charge distribution. The total energy of a molecule with a given set of atomic coordinates was calculated on the basis of the sum of inidividual interatomic interactions (comp = compression; dip = dipole; tor = torsion; vdw = Van der Waals):

$$E_{tot.} = E_{comp} + E_{bend} + E_{vdw} + E_{dip} + E_{tor}$$

These interaction energies were defined as in the Allinger–Yuh program.[29] Minimization of the X-ray coordinates with our force field resulted in no significant shifts in relative atomic positions, indicating a

(23) The mixing of bonding and nonbonding d-orbital characters is not a first-order concern in nonradiative relaxation processes of (^{2}E)Cr(III), but it is important for some possible excited-state quartet relaxation channels and it could make a perturbational contribution to (^{2}E)Cr(III) relaxation rates. On the other hand, admixtures of p-orbital character, induced by the trigonal distortion, would tend to relax the Laport restriction on ^{2}E excited-state relaxation. Consequently, an alternative to the simple surface crossing model, presented below, would be to treat the effect of trigonal distortions as vibronic perturbations, which increase the numerical value of the electronic matrix element for the $^2E_g \rightarrow {}^4A_{2g}$ transition. This approach will be discussed elsewhere.

(24) Ceulemans, A.; Bongaerts, N.; Vanquickenborne, L. C. *Inorg. Chem.* **1983**, *36*, 927.

(25) Abbreviations: sen = 4,4′,4″-ethylidynetris(3-azabutan-1-amine); [9]-aneN$_3$ = 1,4,7-triazacyclononane; TAP[9]aneN$_3$ = 1,4,7-tris(aminopropyl)-1,4,7-triazacyclononane; TAE[9]aneN$_3$ = 1,4,7-tris(aminoethyl)-1,4,7-triazacyclononane; [([9]aneN$_3$)CH$_2$–]$_2$ = 1,2-bis(1,4,7-triaza-1-cyclononyl)ethane; [14]aneN$_4$ = 1,4,8,11-tetraazacyclotetradecane.

(26) Geue, R. J.; Searle, G. H. *Aust. J. Chem.* **1983**, *36*, 927.

(27) Schwarz, C. L. Unpublished results.

(28) Perkovic, M. W. Ph.D. Dissertation, Wayne State University, 1990.

(29) Allinger, N. L.; Yuh, Y. H. Quantum Chemistry Program Exchange, Indiana University, Bloomington, IN; Program No. 395.

(30) (a) Brubaker, G. R.; Johnson, D. W. *Coord. Chem. Rev.* **1984**, *53*, 1. (b) DeHayes, L. J.; Busch, D. H. *Inorg. Chem.* **1973**, *12*, 1505.

Table II. Fractional Atomic Coordinates for [Cr(sen)]Br_3

atom	x	y	z
Br1	1.0567 (1)	−0.2080 (1)	0.06120 (9)
Br2	0.4026 (1)	−0.1412 (2)	0.0737 (1)
Br3	0.1376 (1)	0.1256 (2)	0.2408 (1)
Cr1	0.8053 (2)	0.0247 (2)	0.1963 (1)
N1	0.8771 (7)	0.1921 (9)	0.1857 (6)
N2	0.8063 (8)	−0.016 (1)	0.0403 (6)
N3	0.9341 (7)	−0.0683 (9)	0.2431 (7)
N4	0.6819 (7)	0.132 (1)	0.1708 (6)
N5	0.8009 (7)	0.0387 (9)	0.3553 (6)
N6	0.7210 (7)	−0.1321 (9)	0.1933 (6)
C1	0.803 (1)	0.287 (1)	0.1491 (9)
C2	0.713 (1)	0.262 (1)	0.1964 (9)
C3	0.9597 (9)	−0.052 (1)	0.3593 (9)
C4	0.868 (1)	−0.058 (1)	0.4056 (8)
C5	0.769 (1)	−0.142 (1)	0.0203 (8)
C6	0.684 (1)	−0.161 (1)	0.0812 (8)
C7	0.5991 (9)	0.093 (1)	0.2228 (9)
C8	0.7040 (9)	0.035 (1)	0.3896 (8)
C9	0.6418 (9)	−0.133 (1)	0.2586 (8)
C10	0.6219 (9)	−0.005 (1)	0.3067 (8)
C11	0.528 (1)	−0.020 (1)	0.3585 (9)

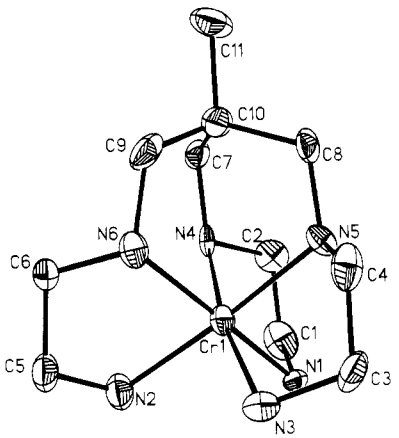

Figure 3. ORTEP diagram at 50% probability of the cation $Cr(sen)^{3+}$.

reasonable basis set for our model. The N–Cr–N bending constraint was then relaxed to determine the geometry preferred by the sen ligand if it were to encapsulate a sphere the size of a Cr(III) ion. The steric energy of the ligand was calculated for different trigonal twist angles by redefining the "unstrained" angles around the Cr atom. Once a minimized structure was found for a given set of input parameters, all contributions of the Cr atom were subtracted from the total steric energy. Details of the calculation method may be found elsewhere.[31]

Single-crystal X-ray diffraction data were collected on a Nicolet R3 diffractometer with Mo Kα radiation (λ = 0.710 73 Å) and a graphite monochromator at ambient temperature. Details of the crystallographic experiment are given in Table I. The molecule crystallized as thin plates in the monoclinic $P2_1/c$ (No. 14) space group. The structure was solved by Patterson methods and refined in a full matrix with the programs of SHELX-76.[32] All non-hydrogen atoms were refined anisotropically. Hydrogen atoms were placed in a combination of observed and calculated positions and held invariant. No correction for extinction was made. Neutral-atom scattering factors were used with the exception of Br^-. These along with the corrections for anomalous dispersion were from ref 33. Absorption corrections were by empirical methods.[26] Lattice constants were derived from 25 high-angle ($2\theta \geq 20°$) reflections and constrained to be monoclinic. A final difference map showed maximum electron density of +0.75 e $Å^{-3}$ near the Cr atom.

Results

The fractional coordinates found for [Cr(sen)]Br_3 are listed in Table II; the bond lengths and bond angles are listed in Table III. A diagram of the cation is shown in Figure 3. Chemically equivalent bond length averages are given in Table IV. The N–Cr–N bite angles average 84.0 (4)°. The Cr–N–C angles in the cap are larger than those in the chelate portions of the

Table III. Bond Lengths (Å) and Angles (deg) for [Cr(sen)]Br_3

Cr1–N1	2.08 (1)	N5–C4	1.49 (2)
Cr1–N2	2.081 (7)	N5–C8	1.49 (2)
Cr1–N3	2.07 (1)	N6–C6	1.51 (1)
Cr1–N4	2.06 (1)	N6–C9	1.49 (1)
Cr1–N5	2.087 (7)	C1–C2	1.50 (2)
Cr1–N6	2.06 (1)	C3–C4	1.49 (2)
N1–C1	1.48 (2)	C5–C6	1.53 (2)
N2–C5	1.47 (2)	C7–C10	1.52 (2)
N3–C3	1.51 (1)	C8–C10	1.52 (2)
N4–C2	1.50 (2)	C9–C10	1.55 (2)
N4–C7	1.48 (1)	C10–C11	1.57 (2)
Cr1–N1–C1	107.5 (8)	N3–Cr1–N5	83.8 (3)
Cr1–N2–C5	108.3 (6)	N3–Cr1–N6	94.5 (4)
Cr1–N3–C3	107.9 (7)	N3–C3–C4	108.0 (9)
Cr1–N4–C2	106.4 (7)	N4–Cr1–N5	88.6 (3)
Cr1–N4–C7	117.3 (7)	N4–Cr1–N6	89.6 (4)
Cr1–N5–C4	106.1 (6)	N4–C2–C1	108.0 (9)
Cr1–N5–C8	117.1 (6)	N4–C7–C10	115 (1)
Cr1–N6–C6	107.6 (6)	N5–Cr1–N6	88.8 (3)
Cr1–N6–C9	117.6 (8)	N5–C4–C3	108.5 (9)
N1–Cr1–N2	92.6 (4)	N5–C8–C10	114.8 (7)
N1–Cr1–N3	91.9 (4)	N6–C6–C5	107 (1)
N1–Cr1–N4	84.5 (4)	N6–C9–C10	115 (1)
N1–Cr1–N5	95.0 (3)	C2–N4–C7	112.5 (8)
N1–Cr1–N6	172.9 (4)	C4–N5–C8	113.3 (8)
N1–C1–C2	109.3 (9)	C6–N6–C9	112.0 (9)
N2–Cr1–N3	93.3 (4)	C7–C10–C8	112 (1)
N2–Cr1–N4	94.8 (4)	C7–C10–C9	110.8 (8)
N2–Cr1–N5	172.0 (4)	C7–C10–C11	106 (1)
N2–Cr1–N6	83.9 (4)	C8–C10–C9	112 (1)
N2–C5–C6	108.2 (9)	C8–C10–C11	108.4 (8)
N3–Cr1–N4	171.3 (3)	C9–C10–C11	107 (1)

Table IV. Structural Comparison (Å and deg) for Three Related Cr Complexes

	$[Cr(en)_3]^{3+}$ [a]	$[Cr(sen)]^{3+}$ [b]	$[Cr(diamsar)]^{3+}$ [c]
Cr–N	2.08 (2)	2.07 (1)	2.073 (6)
N–C	1.49 (43)	1.49 (1)	1.499 (7)
C–C(en)	1.48 (3)	1.51 (2)	1.513 (5)
C–C(ethylene, cap)		1.53 (2)	1.535 (4)
N–Cr–N(bite)	82.3 (8)	84.0 (4)	84.1 (1)
Cr–N–C(cap)		117.3 (3)	116.8 (7)
Cr–N–C(en)	109.5 (1.4)	107.3 (9)	107.4 (7)

[a] There have been many structural determinations of $[Cr(en)_3]^{3+}$. These parameters were averaged from the hits obtained by the Cambridge Structural Database: Allen, F. H.; Kennard, O.; Taylor, R. *Acc. Chem. Res.* **1983**, *16*, 146. Reported structures of $[Cr(en)_3]^{3+}$ that were cocrystallized with $[Co(en)_3]^{3+}$ were omitted from the tabulation as were structures with $R > 8\%$. [b] This work. [c] Comba, P.; Creaser, I. I.; Gahan, L. R.; Harrowfield, J. M.; Lawrance, G. A.; Martin, L. L.; Mau, A. W. H.; Sargeson, A. M.; Sasse, W. H. F.; Snow, M. R. *Inorg. Chem.* **1986**, *25*, 384.

Table V. Absorption and Emission Spectra Data for (Hexaam(m)ine)chromium(III) Complexes

complex	abs max[a] λ, nm (ε, M^{-1} cm^{-1})	emission max[b] λ, nm
$Cr([9]aneN_3)_2^{3+}$	340 (64), 439 (88)[c]	678
$Cr([9]aneN_3CH_2-)_2^{3+}$	360 (142), 481 (280)[d]	710–730[e]
$Cr(sen)^{3+}$	347 (65), 451 (97)	675
$Cr(TAP[9]aneN_3)^{3+}$	352 (325), 462 (267)	671
$Cr(TAE[9]aneN_3)^{3+}$	358 (198), 467 (264)	690
$Cr(en)_3^{3+}$	351 (86), 451 (70)	668
$Cr(NH_3)_6^{3+}$	346 (37), 462 (44)	657
$Cr([9]aneN_3)(NH_3)_3^{3+}$	353 (60), 460 (78)	675[g]

[a] In H_2O except as indicated. [b] Zero-zero line at 77 K in DMSO–H_2O glass. [c] Wieghardt, K.; Schmidt, W.; Hermann, W.; Küppers, H. J. *Inorg. Chem.* **1983**, *22*, 2953. [d] Wieghardt, K.; Tolksdorf, I.; Hermann, W. *Inorg. Chem.* **1985**, *24*, 1230. [e] Broad, matrix-dependent emission.[6b] [f] Kühn, K.; Wasgestian, F.; Kupka, H. *J. Phys. Chem.* **1981**, *85*, 665. [g] Ryu, C. K. Ph.D. Dissertation, Wayne State University, 1987.

(31) Endicott, J. F.; Kumar, K.; Schwarz, C. L.; Perkovic, M. W.; Lin, W-K. *J. Am. Chem. Soc.* **1989**, *111*, 7411.
(32) Sheldrick, G. M. SHELX-76. University Chemical Laboratory, Cambridge, England, 1976.
(33) *International Tables for X-Ray Crystallography*; Kynoch Press: Birmingham, England, 1974; Vol. 4.
(34) Sheldrick, G. M. SHELXTL. University of Gottingen, Federal Republic of Germany, 1978.

Table VI. Photophysical and Photochemical Data for (Hexaam(m)ine)chromium(III) Complexes

complex	τ_{NH}^{77},[a] μs	τ_{NH}^{298},[b] μs	τ_{ND}^{77},[a] ms	τ_{ND}^{298},[b] μs	$k(T)$,[c] s^{-1}	quantum yield in H_2O (298 K)
$Cr([9]aneN_3)^{3+}$	400[d]	30.2	3.03[d]	30.2[d]	3.3×10^4	$<10^{-3}$
$Cr([9]aneN_3CH_2^-)^{3+}$	50[d]	6.5×10^{-5} [d,e]	0.114[d]	1.1×10^{-5} [d,e]	$\geq 1.5 \times 10^{10}$ [f]	$<10^{-3}$
$Cr(TAE[9]aneN_3)^{3+}$ [g]	114	4×10^{-3} [e]	1.0	4×10^{-3} [e]	2.5×10^8	0.27 ± 0.04[h]
$Cr(TAP[9]aneN_3)^{3+}$ [g]	265	179	4.3	850	9.4×10^2	0.01 ● 0.01[h]
$Cr(sen)^{3+}$	171	1×10^{-4} [e]	2.943		$\geq 1 \times 10^{10}$ [f]	0.10 ± 0.01[h]
$Cr(en)_3$[d]	120[i]	1.2[j]	3.03[i]		8.3×10^5	0.27 ± 0.06[h]
$Cr(NH_3)_6^{3+}$[d]	70[i]	2.2[j]	5.23[d]		4.5×10^5	0.45[e]

[a] In DMSO–H_2O glass. [b] In DMSO–0.01 HCF_3SO_3 solution. [c] $k_{nr} = (\tau_{ND}^{298})^{-1} - (\tau_{ND}^{77})^{-1}$. This quantity represents the thermally activated nonradiative decay rate constant for decay channels *not* mediated by high-frequency vibrational modes. [d] References 5c,d. [e] Extrapolated from temperature-dependent lifetimes in glassy media at low temperatures. [f] Picosecond flash-photolysis experiments suggest that the decay rate constant could be somewhat larger. [g] Reference 17. [h] Based on relative quantum yields using $Cr(NH_3)_6^{3+}$ as reference; errors are 1 SD for three or more determinations. [i] (a) Kühn, K.; Wasgestian, F.; Kupka, H. *J. Phys. Chem.* **1981**, *85*, 665. (b) Mvele, M.; Wasgestian, F. *Inorg. Chem.* **1986**, *119*, 25. [j] Reference 6b.

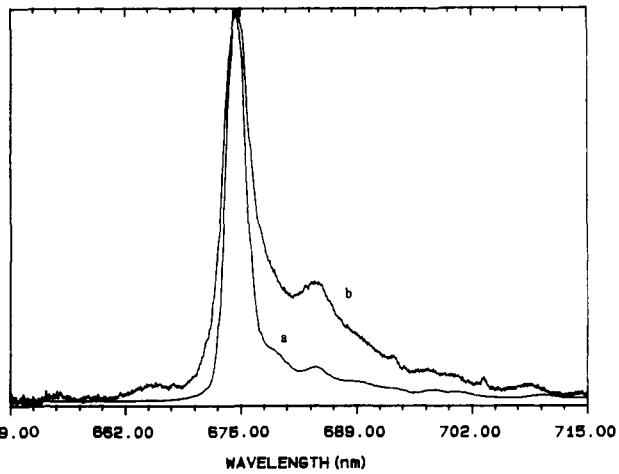

Figure 4. Emission spectra of $Cr(sen)^{3+}$: (a) DMSO–H_2O glass (1:1, v/v) at 77 K; (b) $[Cr(sen)]Br_3$ powder at 300 K.

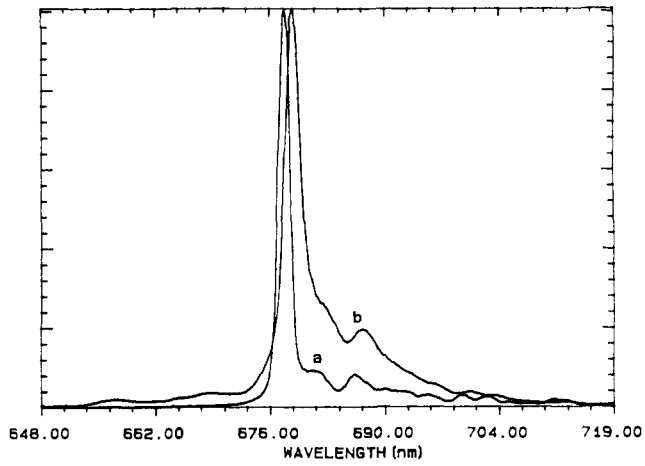

Figure 5. Emission spectra of $Cr(sen)^{3+}$ doped into $[Rh(sen)](ClO_4)_3$ (1:30): (a) at 77 K; (b) at 300 K.

molecule, viz. Cr–N–C(cap) = 117.3 (3)° and Cr–N–C(en) = 107.3 (9)°. The geometry of the cation is entirely normal and as would be predicted from closely related structures in the literature.

The visible–UV spectrum of $Cr(sen)^{3+}$ has absorption maxima that are consistent with expectation for a chromium(III) hexaam(m)ine complex (Table V). The 77 K (^{2}E)Cr(III) emission spectra, with an intense 0-0 line and relatively weak vibronic components, is typical of noncentrosymmetric chromium(III) am(m)ines (Figures 4 and 5). The 0-0 line was somewhat sharper in the solid state (e.g., Figure 4a) at 77 K than in glassy solution or at higher temperatures. The vibronic sidebands were increased in intensity relative to the 0-0 line in the emission spectrum of the doped sample at 300 K as is reasonably typical of these systems, but emissions of fluid solution samples were completely quenched. This is in accord with the dramatic reduction in the (^{2}E)Cr(III) excited-state lifetime in fluid solution (Table VI). The transition to thermally activated decay behavior, as the temperature was increased from 77 K, was also strongly matrix dependent. The lifetime of (^{2}E)$Cr(sen)^{3+}$ doped into $[Rh(sen)](ClO_4)_3$ became temperature dependent at about 263 K with an activation energy of 33 kJ mol^{-1}, while in the DMSO–0.01 M HCF_3SO_3 medium the onset of thermally activated decay occurred at about 180 K (just below the glass–fluid transition region) and E_a = 29 kJ mol^{-1}.

We have included our quantum yield measurements in Table V. The photoaquation yields found for $Cr(sen)^{3+}$ are a little smaller than for $Cr(en)_3^{3+}$, but they are similar to the photoaquation yield ascribed to $(^4T_{2g})Cr(NH_3)_6^{3+}$.[6]

Our molecular mechanics calculations indicate that the sen ligand has a considerable propensity to twist along a trigonal axis. The steric energy of the ligand was calculated for the limiting prismatic and antiprismatic, as well as for the observed and several intermediate geometries. These calculations indicate that the sen ligand had a minimum energy (see Figure 6) conformation with

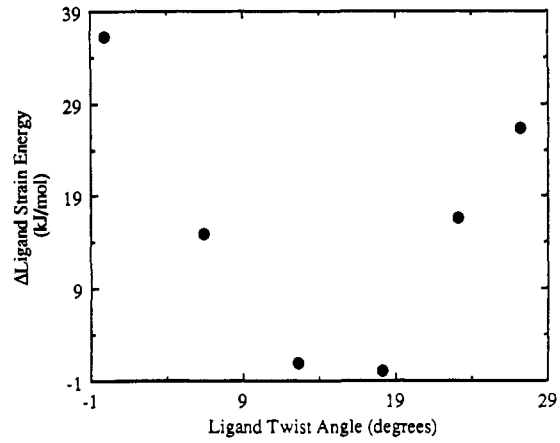

Figure 6. MM2-calculated changes in the steric energy of the sen ligand as a function of the trigonal twist angle.

a twist angle of about 14° (antiprismatic = 30°; prismatic = 0°) when coordinated to a sphere the size of Cr(III). Relaxation of the ground-state geometry (twist angle = 25.4° from the X-ray structure; 26.2° from the MM2 calculations) to this minimum corresponds to a decrease of 18 kJ mol^{-1} in ligand steric energy. The calculations also indicate that the twist angle of the minimum energy ligand conformation would decrease monotonically as the Cr–N bond length is increased (–4.5° for a change of 0.6 Å; this calculation involved variation of the Cr–N equilibrium distance, with the N–Cr–N angle constraints set to 0).

Discussion

This study has demonstrated that the introduction of trigonal strain through the capping of $Cr(en)_3^{3+}$ with a neopentyl moiety facilitates access to an efficient, thermally activated nonradiative relaxation channel for the (^{2}E)$Cr(sen)^{3+}$ excited state in ambient

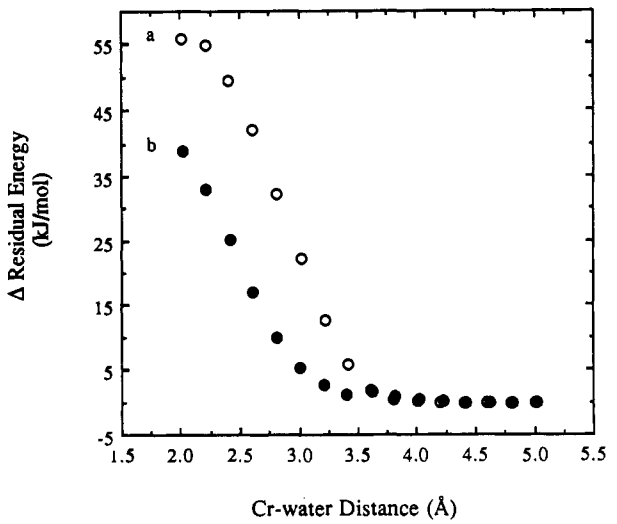

Figure 7. MM2 simulations of steric energy changes that occur when a water molecule approaches the "open" trigonal face of $Cr(sen)^{3+}$: (a) antiprismatic $Cr(sen)^{3+}$ coordination geometry; (b) prismatic $Cr(sen)^{3+}$ coordination geometry. Differences in the residual (ligand only) steric energies are with respect to the limiting steric energies obtained for a Cr–water distance of 5 Å; these energies are 92.1 and 103.3 kJ mol^{-1}, respectively.

solutions. The possible nature of the relaxation is considered below.

This is the second published structural characterization of the sen ligand. The complex $Co(sen)^{3+}$ has been investigated by Yoneda et al.[35] and exhibits the kind of differences expected with the difference in metal ion; i.e., $Co(sen)^{3+}$ has shorter M–N distances (1.971 (6) Å) and larger bite angles (86.1 (2)°) but overall is very similar to $Cr(sen)^{3+}$. A comparison was made between $Co(sen)^{3+}$ and $Co(en)_3^{3+}$ with the conclusion that "capping of the ligand does not affect the structure of the central $Co(en)_3^{3+}$ moiety."[35] Similarly, $Cr(sen)^{3+}$ and $Cr(en)_3^{3+}$ show the same central geometry, and the similarity extends to the doubly capped ligand complex $Cr(diamsar)^{3+}$. Table IV summarizes the geometric parameters for $Cr(en)_3^{3+}$, $Cr(sen)^{3+}$, and $Cr(diamsar)^{3+}$. It would seem that singly or doubly capping the en ligands in this manner produces no substantive change to the $Cr(en)_3^{3+}$ core for the ground-state electronic configuration. This similarity in ground-state molecular structures is consistent with the very similar electronic absorption and emission spectra of these complexes: i.e., the microsymmetries of the Cr(III) centers are nearly identical.

A twist angle θ can be defined[36] to indicate the amount of twist between the two N_3 faces at each end of the en ligand, where θ = 30° describes an octahedral environment for the central ion and θ = 0° indicates a trigonal prism. Twist angles for $Cr(en)_3^{3+}$ have been tabulated by Kepert[28] and range 25.1–26.7°, which is only slightly distorted from octahedral. The $Cr(sen)^{3+}$ complex reported herein shows θ = 25.4°, while $Cr(diamsar)^{3+}$ has θ = 24.5°. The $Co(sen)^{3+}$ is slightly more octahedral with θ = 27.3°, but all these examples are nearly equivalent.

The similarity of ground-state coordination geometries of $Cr(en)_3^{3+}$ and $Cr(sen)^{3+}$ results in very similar electronic structures of these complexes (Table V). Examination of Tables V and VI clearly shows that the most obvious electronic properties of these complexes (e.g., the differences in energy of the lowest quartet and doublet excited states) are not correlated with the spectacular variations found for their ambient lifetimes. However, there is a very strong correlation between the tendency of the ligand to twist along a trigonal axis and the efficiency of the thermally activated decay pathway.

We have noted in the Introduction that a large amplitude trigonal twist might facilitate d–d excited-state relaxation. In order to explore this hypothetical relaxation coordinate more carefully, we have developed a very simple, primitive model,[37] which is qualitatively represented in Figure 8. The limiting distortion along the trigonal twist coordinate generates a trigonal-prismatic CrN_6 geometry. The lowest energy doublet excited state in the trigonal-prismatic geometry (D_{3h}) will have an $(e')^3$ electronic configuration. Simple angular overlap arguments[38] indicate that this $^2E'(D_{3h})$ electronic state would have an energy comparable to that of the $^2E_g(O_h)$ electronic excited state of CrN_6 (note that the $t_{2g}(O_h)$ and the $e'(D_{3h})$ orbitals are largely nonbonding in am(m)ine complexes). Of course the $^4E'(D_{3h})$ state of the trigonal-prismatic complex, with an $(e')^2(e'')$ electronic configuration (see Figure 8A), would be appreciably destabilized relative to the $^4A_{2g}(O_h)$ parent, with its $(t_{2g})^3$ electronic configuration. The simplest model for the twisting coordinate would be one with similar energies and twisting force constants for the $^2E_g(O_h)$ and $^2E'(D_{3h})$ electronic excited states. Then $^2E_g(O_h) \rightarrow {}^2E'(D_{3h})$ surface crossing can be described as a nearly classical surface crossing with the transition state occurring for a 15° twist angle.

We have used molecular mechanics methods to examine the contributions that the relaxation of trigonal strain within the coordinated sen ligand. Our calculations indicate that the sen ligand is trigonally strained in the antiprismatic environment. This ligand centered strain is manifested in larger than normal angles in the neopentyl cap. The relaxation of the ligand from the nearly antiprismatic $(^4A_2)Cr(sen)^{3+}$ geometry to the preferred ligand geometry (14° twist angle) reduces the steric energy of the ligand by an estimated 18 kJ mol^{-1}. If the trigonal relaxation coordinate were the only contribution to $k(T)$ that was different in (^2E)-$Cr(sen)^{3+}$ and in $(^2E)Cr(en)_3^{3+}$, and if the variations in ligand steric energies only affect the energy of the transition state, then $[k(T)]_{en}/[k(T)]_{sen} \sim \exp(\Delta E_{st}/RT)$, and we would predict about a 10^3-fold larger relaxation rate constant for $(^2E)Cr(sen)^{3+}$ than for $(^2E)Cr(en)_3^{3+}$.

The observations on $Cr(sen)^{3+}$ are qualitatively similar to our observations on other complexes containing trigonally strained ligands. Overall, the greater the tendency of the ligand to twist along a trigonal coordinate, the shorter the $(^2E)Cr(III)$ excited-state lifetime in ambient solutions, and when the trigonal twisting pathway is stereochemically restricted, as in $Cr(TAP[9]$-$aneN_3)^{3+}$,[17] or when it is restricted by a rigid-state matrix as in

(35) Okazaki, H.; Sakaguchi, U.; Yoneda, H. *Inorg. Chem.* **1983**, *22*, 1539–1542.

(36) Kepert, D. L. *Inorganic Stereochemistry*; Springer-Verlag: New York, 1982; pp 92–97.

(37) The simple model discussed here is to be regarded as a limiting model, since it seems clear that several relaxation channels can contribute to the thermally activated relaxation of Cr(III) complexes.[5,8,10] In the semiclassical limit the relaxation rate constant for each such channel would be represented at (e.g., see: Newton, M. D.; Sutin, N. *Annu. Rev. Phys. Chem.* **1984**, *35*, 437)

$$k_i = (\kappa_{el})_i(\kappa_{nu})_i(\nu_{nu})_i$$

where $(\kappa_{el})_i$, $(\kappa_{nu})_i$, and $(\nu_{nu})_i$ are the electronic transmission coefficient, the nuclear transmission coefficient, and the characteristic frequency of nuclear motion, respectively, associated with the ith channel. The sum over all channels would give the observed relaxation rate constant, $k(T)$. The very simple model described here presumes that for the relaxation channel involving a trigonal distortion, $\kappa_{el} \sim 1$, $\kappa_{nu} \simeq \exp(\Delta G^*/RT)$, and $\Delta G^* = \Delta G_{tr}^* + \Delta E_{st}^*$, where ΔG_{tr}^* is the nuclear reorganizational energy required to achieve the geometry of the transition state when there is no change of the steric energy (ΔE_{st}^*) of the coordinated ligands. The MM2 parameters that we have used suggest that $\Delta G_{tr}^* \simeq 153$ kJ mol^{-1} for the $(^4A_{2g})Cr(NH_3)_6^{3+}$ ground state. Simple angular overlap considerations (E_σ = 7.18 × 10^3 cm^{-1})[38b] indicate that the $Cr(NH_3)_6^{3+}$ ground state would be destabilized by about 80 kJ mol^{-1} for a 15° twist. These estimates are probably reasonable upper and lower limits. The angular overlap calculations indicate that there would be no loss of stabilization energy for a trigonal twist of $Cr(NH_3)_6^{3+}$ in a doublet electronic configuration with doubly occupied t_{2g} orbitals, but one expects about a 12 kJ mol^{-1} promotion energy to achieve such a configuration. It is likely that the angular overlap approach again underestimates the repulsions for a large amplitude twist in the doublet state, but the estimate that ΔG_{tr}^* is 60 kJ mol^{-1} or so smaller in the ^2E_g than in the $^4A_{2g}$ state of $Cr(NH_3)_6^{3+}$ is in good, qualitative accord with our observations and arguments.

(38) (a) A crude angular overlap calculation assuming similar σ parameters for the amine as for NH_3[38b] indicates that the ground state of a trigonal-prismatic complex would be about 8.6 × 10^3 cm^{-1} less stable than the ground state of an octahedral complex (see Figure 8). (b) Vanquickenborne, L. C.; Ceulemans, A. *Coord. Chem. Rev.* **1983**, *100*, 157.

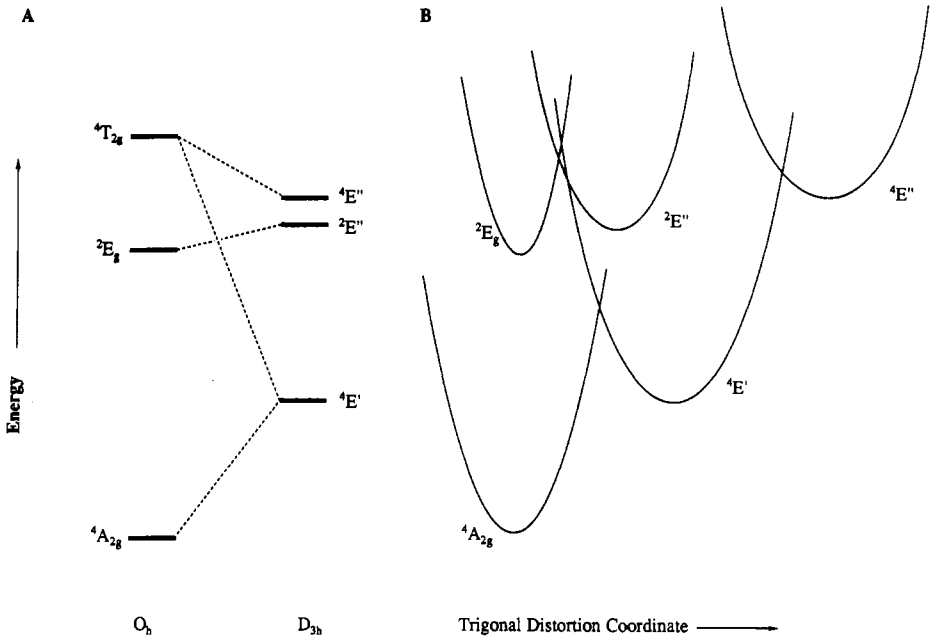

Figure 8. Qualitative correlation of the electronic state energies for octahedral (O_h) and trigonal prismatic (D_{3h}) CrN_6^{3+} complexes (A) and a qualitative representation of the lowest energy excited-state potential energy surfaces for these two geometries (B). The O_h excited-state energies were based on $Cr(NH_3)_6^{3+}$. The D_{3h} state energies are based on an angular overlap calculation that only considered the off-diagonal matrix elements that were larger than 0.5σ. Values of the AOM σ parameters are from ref 32b. The relative displacement of the potential energy surfaces along the trigonal distortion coordinate was based on changes in bond order from the AOM calculation.

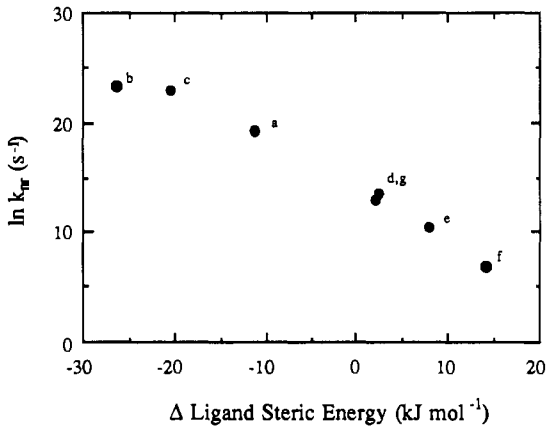

Figure 9. Correlation of the thermally activated nonradiative relaxation rate, k_{nr}, for some chromium(III) chromiumhexaam(m)ine complexes, with change of steric energy within the ligand that is calculated for a trigonal twist from the ground-state geometry to a geometry in which the twist angle is 15°: (a) $Cr(TAE[9]aneN_3)^{3+}$; (b) $Cr[([9]aneN_3)\text{-}CH_2\text{-}]_2^{3+}$; (c) $Cr(sen)^{3+}$; (d) $Cr(NH_3)_6^{3+}$; (e) $Cr([9]aneN_3)_2^{3+}$; (f) $Cr(TAP[9]aneN_3)^{3+}$; (g) $Cr(en)_3^{3+}$.

$Rh(sen)^{3+}$:$Cr(sen)^{3+}$ salts, the resulting (^{2}E)Cr(III) excited state is relatively long-lived (exceptionally long-lived in the case of $Cr(TAP[9]andN_3)^{3+}$). We have illustrated the correlation between $k(T)$ and the steric energy associated with a large amplitude trigonal twist in Figure 9 by means of a comparison of the observed values of $k(T)$ for several (hexaam(m)ine)chromium(III) complexes in ambient solutions (Table VI) with the differences between the ligand's steric energy in the ground-state conformation and in the conformation with a 15° twist angle. It is surprising, and probably a little misleading, that the slope in Figure 9 is approximately $(RT)^{-1}$. At this stage we interpret this good a fit of the primitive model to be qualitative support for the importance of the trigonal twisting motion as a pathway for thermally activated relaxation of (^{2}E)Cr(III) excited states. Work now in progress may lead to a more realistic model of this relaxation pathway.[39] It is to be noted that Figure 9 only demonstrates a general trend in the *relative*, thermally activated nonradiative relaxation rate with one factor, and it does not exclude the possibility that other relaxation channels may contribute to $k(T)$ for some of the complexes considered. The possibility that doublet-to-quartet spin relaxation occurs concomitant with the large amplitude trigonal twisting motion, without an actual $^2E_g(O_h) \rightarrow {}^2E'(D_{3h})$ surface crossing, needs to be considered, but this is beyond the scope of this paper.[40]

While these (hexaamine)chromium(III) complexes were selected for study because they had potential for letting us explore a trigonal twisting coordinate as a pathway for (^{2}E)Cr(III) relaxation with little variation in possible back intersystem crossing pathways, our results do reflect to a limited extent on the other possible relaxation pathway, which is mentioned in the Introduction. Thus, relaxation by means of a chemical reaction pathway would presumably require association between H_2O and the (^{2}E)Cr(III) excited state. It is obvious that partially blocking access of H_2O to the coordination sphere by capping one of the (relatively open) trigonal faces of $Cr(en)_3^{3+}$ with a neopentyl group does not result in a long-lived $Cr(sen)^{3+}$ complex (other problems with this mechanism have been discussed previously[5a,16]). Nevertheless, a thermally induced distortion of the coordination sphere might couple with substitution of an amine by H_2O. This is an important possibility in view of evidence for such a photochemical intermediate in the *cis*-$Cr([14]aneN_4)(NH_3)_2^{3+}$.[41] We have used MM2 simulations to examine the ligand–ligand repulsions that result from associating a water molecule with Cr at the uncapped

(39) Perkovic, M. W.; Ryu, C. K.; Endicott, J. F. Work in progress.

(40) A reviewer has suggested that the contrast in (^{2}E)Cr(sen)$^{3+}$ excited-state lifetimes in fluid H_2O/DMSO solutions and the doped solid might arise from the H_2O association pathway. However, the very large amplitude ligand motions considered here are very unlikely in the solid state. A related precedent for repressing such motions in the solid state is the 3–6 kJ mol^{-1} larger barrier for ligand rotation around the C_5 axis of ferrocene in the solid state[40a,b] than in the gas phase.[40c] The larger solid state barriers to such large amplitude motions presumably arise from the intermolecular, nearest-neighbor interactions in the rigid matrix. The mechanism discussed here would require at least 10 kJ mol^{-1} greater barrier for twisting of the sen ligand along a C_3 axis of Cr(sen)$^{3+}$ in the ionic solid than in solution. (a) Haaland, A. *Acc. Chem. Res.* **1979**, *12*, 415. (b) Maverick, E.; Dunitz, J. D. *Mol. Phys.* **1987**, *62*, 451. (c) Campbell, A. J.; Fyfe, C. A.; Harold-Smith, D.; Jeffrey, K. R. *Mol. Cryst. Liq. Cryst.* **1976**, *36*, 1.

(41) Waltz, W. L.; Lee, S. H.; Friesen, D. A.; Lilie, J. *Inorg. Chem.* **1988**, *27*, 1132.

trigonal face of $Cr(sen)^{3+}$ in its ground-state geometry and in the trigonal-prismatic geometry. The results shown in Figure 7 indicate that such an association is about 17 kJ mol^{-1} less repulsive in the trigonally distorted complex than in the ground state. This suggests that trigonal distortion, at least of $Cr(sen)^{3+}$, could facilitate ligand substitution as well as excited-state relaxation. To the degree that doubly occupied microstates contribute to a (^{2}E)Cr(III) electronic structure in a D_{3h} microenvironment, there could also be a stronger bond between (^{2}E)Cr(III) and the entering group in the D_{3h} than in the O_h geometry, so that association with solvent and the trigonal distortion might interact synergistically to promote the large amplitude trigonal distortions that result in excited-state relaxation. The present information does not allow resolution of such details. Our observations do indicate that the trigonal twist itself (without solvent association) is probably sufficient to induce excited state relaxation and that association with the solvent, if it occurs, may well occur after the electronically excited system is far into the relaxation channel.[42]

(42) Note that the several reports of photoracemization of Cr(III) complexes that have D_3 symmetry[33] could be evidence for very large amplitude of trigonal distortions in (^{2}E)Cr(III) relaxation: (a) Kane-Maguire, N. A. P.; Langford, C. H. *J. Am. Chem. Soc.* **1972**, *94*, 2125. (b) Kane-Maguire, N. A. P.; Langford, C. H. *Inorg. Chem.* **1976**, *15*, 464. (c) Kane-Maguire, N. A. P.; Phifer, J. E.; Toney, C. G. *Inorg. Chem.* **1976**, *15*, 593.

Conclusions. We have shown that introduction of trigonal strain into $Cr(en)_3^{3+}$ by encapsulating one trigonal face with a neopentyl moiety results in many orders of magnitude decrease in the ambient solution ^{2}E excited-state lifetime of the resulting $Cr(sen)^{3+}$ complex. The chromium microenvironments differ very little in the $Cr(en)_3^{3+}$ and $Cr(sen)^{3+}$ complexes, and this structural similarity is reflected in the very similar electronic properties of the two complexes. The one notable difference between them is the tendency of the coordinated sen ligand to twist along a trigonal axis. Thus, these two complexes fit nicely into a pattern of behavior that has begun to emerge for (hexaam(m)ine)chromium(III) complexes: large-amplitude trigonal distortions facilitate thermally activated (^{2}E)Cr(III) excited-state relaxation.

Acknowledgment. We wish to thank the AT&T company for their gift of the 3b2 computers, terminals, and operating software. The X-ray diffractometer was purchased through an NSF equipment grant to Wayne State University.

Registry No. $[Cr(sen)]Br_3$, 134567-53-6; $[Rh(sen)]Cl_3$, 134567-54-7; $[Rh(sen)]Br_3$, 134567-55-8; $Cr([9]aneN_3)_2^{3+}$, 93714-28-4; $Cr([9]aneN_3CH_2^-)_2^{3+}$, 95388-39-9; $Cr(TAP[9]aneN_3)^{3+}$, 125454-25-3; $Cr(TAE[9]aneN_3)^{3+}$, 125454-24-2; $Cr(en)_3^{3+}$, 15276-13-8; $Cr(NH_3)_6^{3+}$, 14695-96-6; $Cr([9]aneN_3)(NH_3)_3^{3+}$, 116745-22-3.

Supplementary Material Available: For $[Cr(sen)]Br_3$, Tables B and C, listing thermal parameters and hydrogen atomic parameters (2 pages); Table A, listing observed and calculated structure factors (23 pages). Ordering information is given on any current masthead page.

Contribution from the Departments of Chemistry, Grinnell College, Grinnell, Iowa 50112, and University of Vermont, Burlington, Vermont 05405

NMR and Crystallographic Determination of Stereoselectivity in the Coordination of Prochiral Olefinic Alcohols in Mixed Olefin–Amino Acid Complexes of Platinum(II)

Luther E. Erickson,*,† Garth S. Jones,† Jason L. Blanchard,† and Kazi J. Ahmed‡

Received August 17, 1990

NMR spectroscopy (^{1}H, ^{13}C, and ^{195}Pt) was employed to determine the effect of metal-centered stereochemistry on the stereoselectivity of coordination of prochiral olefinic alcohols by comparing the equilibrium distribution of diastereomers of cis- and trans(N,olefin) isomers for mixed olefin–amino acid complexes of general formula Pt(amino acid)(olefin)Cl for amino acid = glycine, α-aminoisobutyric acid, sarcosine (sar), and (*S*)-proline (*S*-pro) and olefin = allyl alcohol, 3-buten-2-ol, and 2-methyl-3-buten-2-ol (2-mb). In agreement with earlier reports, the stereoselectivity of olefin coordination is not significant (ratio of diastereomers 1.0–1.3) for any of the trans(N,olefin) species. However, for cis(N,olefin) isomers of N-chiral sarcosine and (*S*)-proline, the stereoselectivity is substantial, especially for 2-mb for which the preferred diastereomers predominate by >40/1. X-ray structures of the preferred isomers of *cis*(*N-olefin*)-Pt(sar)(2-mb)Cl (space group *Pcab* with a = 10.705 (3) Å, b = 13.671 (3) Å, c = 15.908 (3) Å, Z = 8, and R = 0.046), of *trans*(*N,olefin*)-Pt(*S*-pro)(2-mb)Cl (space group $P2_12_12_1$ with a = 6.955 (4) Å, b = 9.971 (4) Å, c = 19.060 (9) Å, Z = 4, and R = 0.069), and of the related dimethyl sulfoxide complex *cis*(*N,S*)-Pt(sar)(Me_2SO)Cl (space group *Pbca* with a = 10.290 (3) Å, b = 12.398 (3) Å, c = 16.231 (6) Å, Z = 8, and R = 0.041) were determined in order to establish the stereochemistry of the preferred isomers (olefin-*R*, amino acid N-*S* in both cases) and to identify intramolecular interactions, including hydrogen bonding, that contribute to the large stereoselectivities observed for cis(N,olefin) species.

Introduction

The asymmetric template available in a metal atom and its attached ligands provides a simple and convenient method for achieving stereoselectivity in the coordination of another chiral or prochiral ligand. Such stereoselectivity of coordination can be exploited in the development of methods for asymmetric synthesis[1] and for separation of isomers,[2] including optical isomers.[3] Though steric factors are no doubt responsible for observed differences in selectivity of binding, the degree of stereoselectivity for the binding of a particular ligand with a given chiral template is difficult to predict with any certainty. This project, part of a systematic study of the interaction between metal-centered and ligand-centered stereochemistry, was undertaken to provide such fundamental data for mixed amino acid–olefin–platinum(II) complexes of general formula Pt(amino acid)(olefin)Cl, which can exist in two stable geometric isomers denoted trans(N,olefin) (**1**) and cis(N,olefin) (**2**).

Saito and co-workers have reported investigations of both stereochemistry and of olefin exchange in several mixed olefin–amino acid complexes by NMR and optical spectroscopy, including

(1) Morrison, J. D., Ed. *Asymmetric Synthesis*; Academic Press: New York, 1985; Vol. 5.
(2) Jacques, J.; Collet, R.; Wilen, S. H. *Enantiomers, Racemates, and Resolutions*; Wiley-Interscience: New York, 1981.
(3) As employed by Cope et al. for the resolution of cyclooctadiene and other chiral olefins: Cope, A. C.; Gaellin, C. N.; Johnson, W. H. *J. Am. Chem. Soc.* **1962**, *84*, 3191. Cope, A. C.; Careso, E. A. *J. Am. Chem. Soc.* **1966**, *88*, 1711.

† Grinnell College.
‡ University of Vermont.

0020-1669/91/1330-3147$02.50/0